fluids

MDPI

Article

Winter Ice Dynamics in a Semi-Closed Ice-Covered Sea: Numerical Simulations and Satellite Data

Ilya Chernov [1,*,†], Alexey Tolstikov [2,†], Vyacheslav Baklagin [2,†] and Nikolay Iakovlev [3,†]

[1] Institute of Applied Math Research, Karelian Research Centre of RAS, 185035 Petrozavodsk, Russia
[2] Northern Water Problems Institute, Karelian Research Centre of RAS, 185035 Petrozavodsk, Russia
[3] Marchuk Institute of Numerical Mathematics of the RAS, 119333 Moscow, Russia
* Correspondence: iachernov@yandex.ru or chernov@krc.karelia.ru
† These authors contributed equally to this work.

Abstract: The White Sea is a small shallow sea covered by ice in winter. There are very few numerical models of this sea. For the ice-free sea, much data has been collected, but for winter only a small amount (satellite data only). We use our finite-element numerical model Jasmine and satellite data to trace the ice advection and exchange between parts of the White Sea. The aim of the investigation is to adjust the model to adequately reproduce the White Sea ice dynamics. By comparing satellite data on sea-ice concentration with the model prediction, we show that the model describes sea-ice dynamics well, and use it to estimate ice flow from bays to the middle part of the sea and ice exchange through the narrow strait. Ice exchange between neighbouring parts of the sea is shown to be intensive, with large dispersion compared to the time-mean, and bays are shown to be ice producers, while the Gorlo straight is shown to accept ice. We demonstrate that the model is a tool that can be used to better understand the winter regime of the sea.

Keywords: White Sea; numerical simulation; sea ice; winter regime; satellite data; currents

Citation: Chernov, I.; Tolstikov, A.; Baklagin, V.; Iakovlev, N. Winter Ice Dynamics in a Semi-Closed Ice-Covered Sea: Numerical Simulations and Satellite Data. *Fluids* **2022**, *7*, 324. https://doi.org/10.3390/fluids7100324

Academic Editors: Alberto Alberello, Marzieh H. Derkani, Swapnadip De Chowdhury, Filippo Nelli, Richard Manasseh and Mehrdad Massoudi

Received: 19 August 2022
Accepted: 7 October 2022
Published: 11 October 2022

1. Introduction

The White Sea is one of the most studied seas in Russia. It was occupied several hundred years ago by a population who settled on the coasts and used the sea to fish and hunt marine animals. Parts of the sea have their own names (Figure 1). Scientific research has been carried out here for about two hundred years. Most expeditions to investigate the area have occurred in the warm period of the year. Due to the complexity of organizing winter expeditions and the winter regime of this reservoir, the ice dynamics and ice rafting have been studied sporadically, mainly at river mouths or at the White Sea biological stations, which are localized in a small area of Kandalaksha Bay.

Nevertheless, these data are extremely important for understanding the volumes and patterns of ice drift and ridging and the functioning of ecosystems, including cryocommunities.

The White Sea is of considerable interest to scientists. The survey [1] (updated and published in Russian in 2007) and the collective monograph [2] summarize the results of interdisciplinary studies of the White Sea. The book [2] summarizes data that has been obtained over several years (since 2007). In recent years, warming has been observed in the Arctic [3,4], including the White Sea [5], so these surveys are somewhat outdated. The ice cover is shrinking and the periods of ice formation and ice destruction are shifting. Consideration of possible changes to the ecosystems is required, with the development of climate warming taken into account. In this regard, it is necessary to have numerical models that adequately describe the situation and are consistent with observational data. To our knowledge, there are no comprehensive studies on the winter regime of the White Sea.

From a numerical simulation viewpoint, the White Sea is a relatively small shallow sea with a complex bathymetry and coastline. Strong tidal sea-level fluctuations result in

high current velocities (up to 2 m/s) and relatively high available potential energy. This imposes strong constraints on the time step due to the Courant–Friedrichs–Lewy condition.

Conditions in the bays are significantly different: some exchange matter and energy with the neighboring areas more actively, others much less. Depths in the bays differ. Some bays are fed by strong rivers, and river discharge plays an important role, because rivers bring 4% of the sea volume annually [1]. Due to this, the salinity of the White Sea is lower than in the neighboring Barents Sea, and varies significantly over the sea. Fresh water is also responsible for stratification, which is difficult to reproduce in the model. A key feature needing description is the active mixing that occurs due to tidal dynamics.

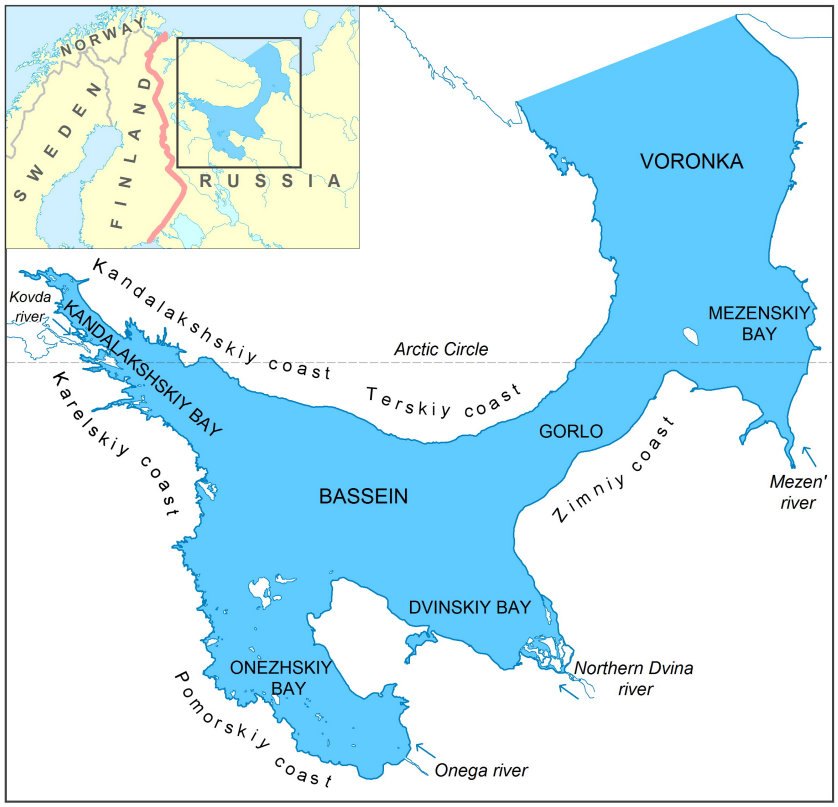

Figure 1. Parts and coasts of the White Sea. Areas of the parts are (thousand km^2): Voronka 24.6, Gorlo 10.2, Mezenskiy Bay 5.6, Bassein 21.8, Dvinskiy Bay 9.6, Onezhskiy Bay 12.3, Kandalakshskiy Bay 6.5.

The authors developed and support a comprehensive numerical model of the White Sea, called Jasmine, which is described in more detail below in Section 2.3. The purpose of the study was to adjust the thermohydrodynamic block of the Jasmine model to adequately reproduce the dynamics of ice cover in the White Sea.

Studying sea ice is important. It has been less studied than the currents, thermohaline dynamics, etc, and it is harder to perform in situ measurements. Ice in the White Sea is seasonal: it melts in late spring and starts to appear in late autumn, and can carry matter from one part of the sea to another. It is important to tune the model so that it can predict ice distribution, thickness, amount, and presence in certain locations. The response of the sea to climate change is also of interest; for example, late ice appearance might be a threat to seals that need ice to breed, because they keep their pups on ice floes. Moreover, sea ice has been recognized as a sensitive indicator of changes to the climate.

Therefore, better understanding of sea-ice behaviour in the White Sea would be useful for planning winter expeditions, winter navigation, and management of the marine ecology and aquaculture.

We describe the state-of-the-art in Section 2.3; we note that there is a lack of comprehensive models of the White Sea.

2. Materials and Methods

2.1. Winter Currents and Approaches to Estimating Them

In winter, it is quite difficult to measure the currents, as navigation is difficult for large ships, and is not possible for small ones. Automated data collection in the White Sea and the use of Doppler current-velocity meters are prohibited by restrictions imposed by the Ministry of Defense. Data collected by submarines are not available. Only observations from scientific stations are available; unfortunately, there are very few of them in the White Sea and almost all are concentrated in a small section of the coast and islands of Kandalakshskiy Bay. These sources are insufficient to describe the movement of ice in winter.

The only approach possible is numerical simulation, but any model requires data-based verification. One possibility is to track the motion of ice and the exchange of ice between parts of the sea. Satellite images are most suitable for model verification. Nevertheless, there are also some difficulties with these, since for about 200 days a year there is an increased amount of cloud over the White Sea.

The tidal currents form a stable pattern. The northern part of the sea is separated from the southern part by the relatively narrow and shallow strait referred to as Gorlo; it prevents penetration of the induced tidal wave to the southern part of the Sea. Thus, in the northern part of the sea, tidal currents are strong, and the tide can be up to 10 m high. To the south of Gorlo, the currents are weak, with the exception of certain local areas in Kandalakshskiy Bay, and the tide is 1.5–2 m. A constant flow is directed from Dvinskiy Bay to Gorlo and travels further along the Zimniy coast to Voronka. From Voronka into Gorlo, waters of another constant current flow and are directed along the Terskiy coast to Kandalakshskiy Bay.

The general pattern of both the residual and thermohaline currents in the White Sea reflects counterclockwise movement of the water mass. It is complicated by the complex configuration of the sea, the rugged coastline, and the local features of bays. In addition, there are quasi-permanent eddies and frontal zones in the White Sea.

Since the intensity of both thermohaline currents in the White Sea strongly depends on river runoff, they exhibit seasonal dynamics. The summer currents have been studied much more than the winter currents.

We know that water flux out of the bays in summer is very close to the river runoff, if averaged over days or for longer time periods. Precipitation and evaporation are very close to each other, so the flux from above is negligible (this is stated in [1] and our simulation results agree with this). In winter, snow might accumulate on ice and does not influence water exchange. Tidal motion brings water in and out of the northernmost part of the sea called the Voronka, though the daily balance is close to zero. Temperature, salinity, and passive tracers are carried by the tidal waves, but the amounts of water that are transported there and back are almost the same. On the other hand, the incoming and outgoing flows are affected by different shores, due to the Coriolis force, for example, so the water exchange pattern is of interest.

We sought to study the water exchange between parts of the sea in winter using numerical simulation and satellite data, comparing the results. Ice is a visible marker, so we used sea-ice concentration dynamics. The model used is able to separate ice change due to melting and freezing and ice advection, which is of intrinsic interest.

2.2. Estimating Sea-Ice Concentration in the White Sea

A complete assessment of the dynamics of the ice situation in seas can only be undertaken using satellite data, which are able to cover a much greater area compared to visual observations from stationary observation stations. Microwave-range instruments used on

satellites can also take measurements 24 h a day irrespective of the cloud cover: this is crucial when studying vast areas of seas [6–9].

According to [10–13], satellite microwave passive sensor data from November 1978 to the present were used for monitoring and assessing changes in the ice cover of the Arctic Ocean. The authors of [14] stated that such data are optimal for these tasks, i.e.,the analysis and assessment of the multiyear variability of ice cover in the Arctic Ocean. Therefore, in this study, we also used satellite microwave passive sensor data provided by the National Snow and Ice Data Center NSIDC (https://nsidc.org/data/G02135/versions/3, accessed on 18 August 2022).

Calculations of the sea-ice extent and concentration from the passive satellite data based on microwave brightness temperature were available from October 1978. The first data were obtained using the scanning multichannel microwave radiometer (SMMR) Nimbus-7, and, since August 1987, using a series of special sensor microwave imager (SSM/I) and special sensor microwave imager/sounder (SSMIS) radiometers on defense meteorological satellite program (DMSP) satellites (Table 1).

These satellite data were available as daily-averaged fields of ice concentration in the polar stereographic projection with a cell size of 25×25 km^2 and a time resolution of two days from 26 October 1978 to 20 August 1987, and of one day from 21 August 1987 to the present.

Because ice processes in the White Sea have spatial heterogeneity due to factors such as strong winds and interactions with the Barents Sea [15], we estimated ice conditions for the parts of the Sea (Figure 1). The sea was divided into bays and other parts according to the description provided in [16]. This made it possible to identify spatial and temporal patterns of the ice regime in the White Sea.

Table 1. Radiometers and satellites used in several time spans.

Satellite, Radiometer	Time Span
Nimbus-7 SMMR	26 October 1978–20 August 1987
DMSP-F8 SSM/I	21 August 1987–18 December 1991
DMSP-F8 SSM/I	19 December 1991–29 September 1995
DMSP-F13 SSM/I	30 September 1995–31 December 2007
DMSP-F17 SSMIS	1 January 2008–31 December 2020
DMSP-F18 SSMIS	1 January 2021–up to now

2.3. The Numerical Model

Phenomena in the White Sea have been numerically simulated much less often than, for example, the neighboring Baltic Sea (see, e.g., [17–19] and an old, but still interesting, paper [20]). A fairly complete overview of the models of the White Sea is given in [1] but there are no more recent surveys.

An operational monitoring system [1,21] is actively used for short-time forecasts. Its main drawback is that ice is not included (so it is a summer-only model) and only a part of the Sea is considered.

I.A. Neelov's [1] numerical model is currently not supported.

The ocean-sea ice-biogeochemical model Jasmine [22] is based on the coupled ocean-sea ice model FEMAO (finite-element model of the Arctic Ocean, Iakovlev [23]) and the biogeochemical model BFM [24]. Discretization, numerical schemes, and other details for solving the equations are described in [23]. Adaptation of the model for the White Sea is reported in our paper [22], and parallel implementation is described in [25].

FEMAO is a primitive equation model of the Arctic Ocean with a standard set of approximations, such as Boussinesq, incompressibility and hydrostatics, a linearized free upper surface, 2.5-level Mellor–Yamada [26] with surface-wave parameterization [27,28], diffusion on isoneutral surfaces (according to [29]) and Gent–McWilliams [30] eddy-induced transport with a spatially variable coefficient [31]. Note, that eddy-induced transport is

important even in the case of relatively fine model horizontal resolution due to the small Rossby radius of deformation (about 1 km [32]). The length scale in the parameterization [31] is set to be equal to the mean model horizontal mesh size. The background coefficient of the diffusion of scalars (temperature, salinity and biochemical characteristics) is 0.05 m^2/s. The horizontal viscosity can be parameterized by two schemes: by the vector Laplace operator on a sphere with constant coefficient 0.1 m^2/s, and by the biharmonic operator, with the constant viscosity coefficient, scaled in a proper manner to effectively dump the two-step numerical mode. The governing equations are described in the Supplementary. In the present study, focusing mainly on sea-ice modeling, the first approach was applied, i.e., the vector Laplace operator on a sphere. A detailed comparison of the two parameterizations is beyond the scope of the paper.

Tides induced by the incident wave from the Barents Sea are extremely important for the White Sea because they produce both of the relatively strong residual currents [1], and induce the essential vertical mixing of shallow waters, producing tidal fronts. In this model, tides are described as a harmonic oscillation on the dominant M_2 frequency of the sea level; the boundary condition by Flather [33] is imposed for the velocity. The solar radiation spectrum is split into two bands: short-wave and long-wave, decaying exponentially with the depth scales 1.2 m and 28 m, and occupying 68 and 32% of the spectrum, respectively. Snow on ice is assumed to completely block the light.

The numerical scheme is close to the well-documented FESOM [34] with some minor differences, except for the horizontal grid. The FEMAO horizontal grid is regular, with constant steps in the angular metric (which correspond to about 3 km in both directions). Unlike the model of the Arctic Ocean, where the axes are rotated, we use geographic coordinates, because the Pole is out of the area and the sea is quite small, so that the grid is not degenerate and the grid elements are of more or less equivalent area. The vertical grid horizons (there are 41) have a step of 5 m up to a depth of 150 m and then 10 m. The time step is 6 min, mainly due to high tidal current speed.

The primary consideration of the paper is the setup of the sea-ice model. the main aspects of the dynamics and thermodynamics are similar to the FESIM 2 model [35] (N. Iakovlev is one of the authors). It is also based on elastic-viscous-plastic rheology, but the physical formulation is more sophisticated; there are several ice-thickness gradations, and the ice-thickness redistribution, ridging and ice-strength schemes are more physically consistent and follow the Los Alamos Laboratory CICE model [36]. An ensemble of ice floes is described by the distribution of the probability of meeting an ice floe of the given thickness; this distribution is approximated by a discrete distribution, with 14 gradations of thickness. The sea-ice concentration (also called the compactness) is this probability. It can also be understood as the area covered by the ice of a given thickness relative to the grid cell area. These values are 0.1, 0.2, 0.3, 0.5, 0.7, 1, 1.5, 2, 3, 4, 5, 6, 10 m. As the White Sea ice thickness is generally less than in the Arctic Ocean, some tuning parameters of the ridging scheme were optimized.

The transport of snow and ice by ice drift (in terms of both mass and concentration for each ice-thickness gradation) is calculated by the finite-element flux corrected Taylor–Galerkin scheme (FCT-TG) [37], which guarantees the positiveness of the solution (this scheme is also used for ocean scalars, such as temperature and salinity, and biochemical parameters, if required).

The sea-ice thermodynamics are described locally for each ice-thickness gradation by a zero-dimensional model similar to that of Semtner [38], but with some modifications to the numerical scheme for solving the surface temperature [39], and a parameterization for melt ponds and snow-on-ice distribution added to the albedo scheme [23].

If there is no snow, the penetration of solar radiation with an exponentially decaying depth scale of 1.5 m is imposed.

The choice of a zero-dimensional model was due to the relatively thin seasonal ice all over the White Sea with a typical value of 0.5 m, which is recommended to be treated as ice of no heat capacity and with a linear temperature profile (see [36]).

The general setup of the model is traditional for sea models forced by the atmosphere and rivers (examples include the AOMIP: Arctic Ocean Model Intercomparison Project, or the CORE-II: Coordinated Ocean-ice Reference Experiment, Phase 2). Although sea-ice dynamics are nonlinear, the large-scale response (time- and space-averaged) is assumed to be mainly deterministic, so we need no ensemble runs. The averaging is determined by satellite data for one or two days, and over 25 km. This is more than inertial oscillations and much more than the 1–2 km Rossby radius which are typical for the White Sea. The model resolution is 3 km; thus, the part of the mesoscale eddies spectrum is treated parametrically by the horizontal diffusivity, as discussed above [29,30]. With a 3 km spatial resolution, the sea-ice dynamics can be treated as stable (except for very special and fast cases of ridging); this is confirmed by long-time experience, not only with this model, but with many climate and weather-forecast models across the world. The model numerics are based on well-documented numerical schemes and iterative solvers and the past set of tests, and have already been used to reproduce the observed White Sea circulation and temperature and salinity, so it is anticipated that the final results would be relevant.

Atmospheric forcing is given by 6-h NCEP reanalysis data [40] for the following variables: air temperature at 2 m, air pressure at sea level, humidity, cloud cover, precipitation, and wind speed at 10 m. The components of turbulent and radiation heat fluxes, and of momentum fluxes, are computed according to the AOMIP (Arctic Ocean Model Intercomparison Project) protocol. The reanalysis data were linearly interpolated on the model grid. Unfortunately, the horizontal resolution of the NCEP data is two degrees; thus, only a few data grid points are available in the study area with no local features generated by orography and sea-land contrasts.

At the White Sea–Barents Sea interface, the climatic monthly mean temperature and salinity fields were specified for the cases of inflow and free outflow of the model temperature and salinity.

Rivers play an important role in White Sea dynamics due to the salinity contrast. There are six rivers taken into account with specified multiyear monthly mean runoffs. The treatment of rivers is by virtual flux similar to MOM4.1 [41]. The salinity and temperature of each river is a matter of tuning. The sources of data are collected and discussed in our survey [42].

3. Results and Discussion

We simulated the White Sea dynamics for ten years from 2008 to 2017. Sea-ice concentration can change due to melting/freezing and due to advection, when the ice is taken out of the chosen domain. The model reproduces these processes and can separate them. Ice advection is calculated via two-dimensional divergence. We use the routine for finite-element numerical integration (and the Gauss theorem) to obtain the flux of the sea ice (in terms of relative area) out of the arbitrary domain. We did this for the parts of the sea and obtained the results presented in (Figure 2). The black curve shows the area of ice taken out of the region (so negative values correspond to ice inflow); the red horizontal line represents the time average.

For the whole sea and the river-fed bays, the average ice flux is out of the domain, with complex oscillations in time. There are several days in a row with positive balance (more ice taken out than brought in), then a day or two of negative balance, then a positive balance again.

The time-average flux (the red horizontal line) shows the difference between the amount of ice that appears and melts within the domain. Zero flux means that some ice comes in, some ice (the same or other) leaves, but by summer there is no ice anyway. Some regions might destroy ice that has frozen elsewhere.

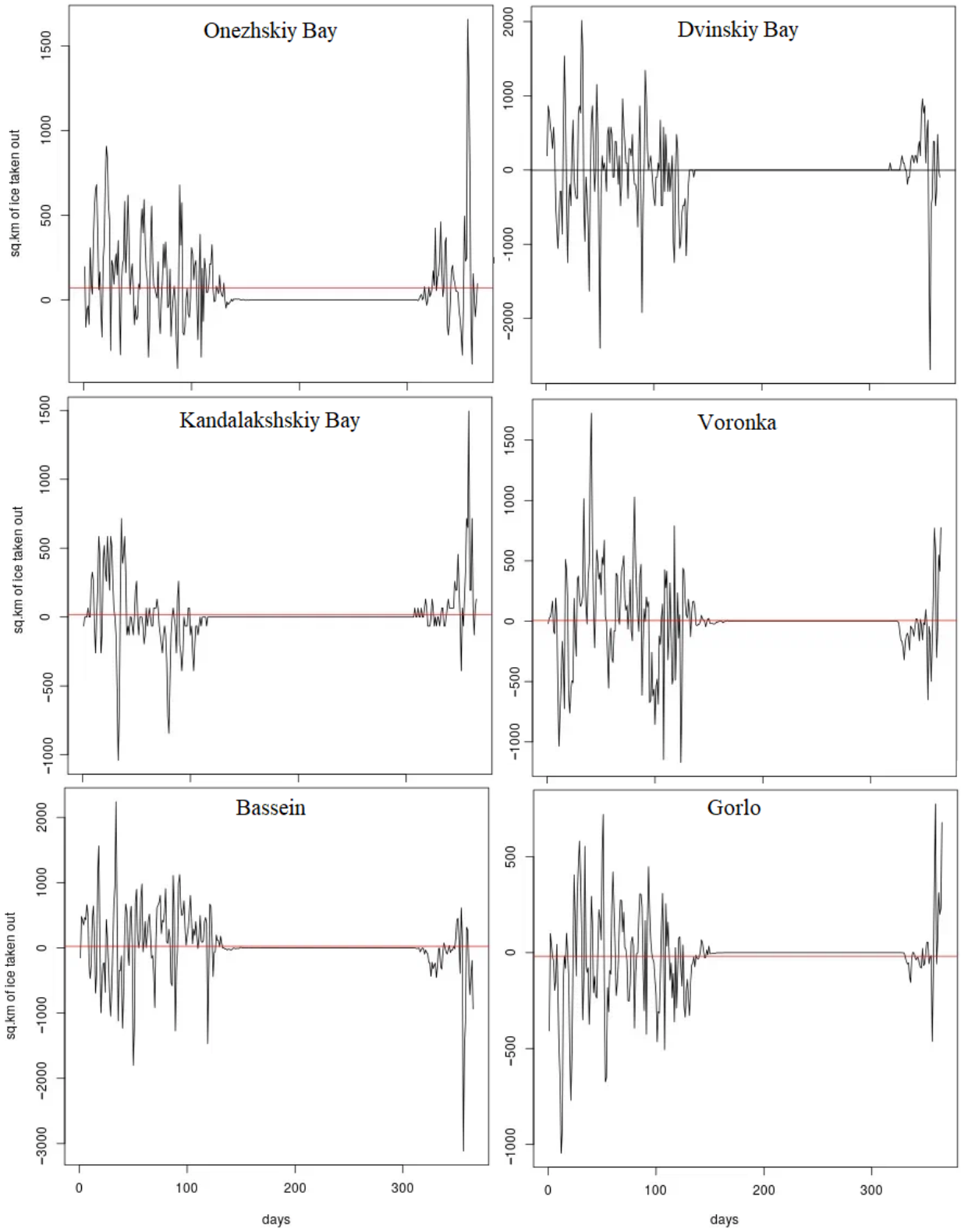

Figure 2. The ice carried out of (positive values) and into (negative values) the sea region during a year, km^2; the red line is the time average.

Kandalakshskiy Bay has almost zero average flux, though several streams feed it. Some ice comes from the Bassein (the middle part of the Sea) to the Bay and the same amount of ice leaves it. Voronka, the region that contains the inter-sea boundary, also has zero average flux. The boundary condition assumes that, at the other side of the boundary,

the sea-ice concentration is exactly the same (zero normal derivative assumption), but the total sea balance is positive. This means that Gorlo and Mezenskiy Bay provide some ice. Gorlo, the narrow strait between two parts of the White Sea, is the only part with negative balance, so it receives (a little) more ice than leaves it. As we have seen, it supplies ice to the Voronka, so it consumes ice from the White Sea core, which, in turn, collects ice from two river-fed bays, Onezhskiy and Dvinskiy. Gorlo is narrow, so the ice there is stuck. The plot shows that, at the beginning and end of winter, negative balance dominates. The first effect is a consequence of the general outflow of the Sea and the ice-filled Gorlo. New ice is just transported to the strait and increases the concentration there. In spring, however, the river discharge becomes stronger, the ice melts and ice from the bays and the core is transported to the Gorlo to melt there. There is a short time (about one week) before complete melting of the ice, where the outflow is more than inflow; during this week, the remaining ice is transported out of the Gorlo.

The figure supports the statement that the ice transfer between the parts of the sea in spring is of the greatest practical interest.

The model is able to evaluate the amount of freezing/melting ice. For the whole sea, the balance is, as we already know, positive; more ice appears than melts, because some ice flows out of the sea. In Figure 3, we show ice melting/freezing. These lines were obtained by numerical differentiation of the sea-ice concentration and subtracting the pure advection. Such large oscillations are due to ridging, which can make the ice thicker, reducing the ice area. It can be seen that, during the quick-melting season, the daily melt is about 5–6% (>4000 km^2) of the sea area (90,000 km^2), while in separate parts, it is much more: 10% in Dvinskiy bay (1000 km^2 compared to 9600 km^2), 30% in Gorlo (1500 km^2 to 10,200 km^2), and about 10% in Kandalakshskiy bay. This agrees well with the satellite observations.

Analysis of the NSIDC satellite data showed that at the beginning and end of the ice period in the White Sea, sea-ice concentration changes drastically (10–12%); this produces jump-like noise in the plot (Figure 4) when the ice freezes and when it actively melts. For parts of the sea, this phenomenon is strong in Kandalakshkiy Bay (about 40 per day) and also (but less so) in Onezhskiy Bay (up to 17–19% per day). In our opinion, this is due to the limitations of the NASA Team algorithm used. In particular, processing land-sea boundary pixels in domains with complex coastlines might cause errors due to incorrect pixel classification. Unfortunately, the available documentation for the data we used (https://nsidc.org/data/G02135/versions/3, accessed on 18 August 2022), provided by NASA, does not describe how the algorithm processes the boundary pixels.

In Figure 4, the daily sea-ice concentration for the whole White Sea for the time-span 2008–2017 and about one year (days 1000–1500, starting from 1 January 2008) is compared. The plots show that the model closely agrees with the satellite data. Using the popular mean-square criterion

$$N^{-1}\sqrt{\sum_i \frac{(x_i - y_i)^2}{(y_i + 1)^2}},$$

we get 0.09 (here N is the size of the sample,and x and y are two vectors of model values and the observations). The worst possible value for the probability-type quantities (between 0 and 1) is 1 (if x is constant 1 and y is constant 0). For the random vectors of the same size the value is close to 0.3. The linear regression is significant at a trust level of at least 10^{-8}, with $R^2 = 0.86$. The same is true for the parts of the sea. The north-western Kandalakshskiy Bay is worse than other parts of the sea. The reasons are discussed above.

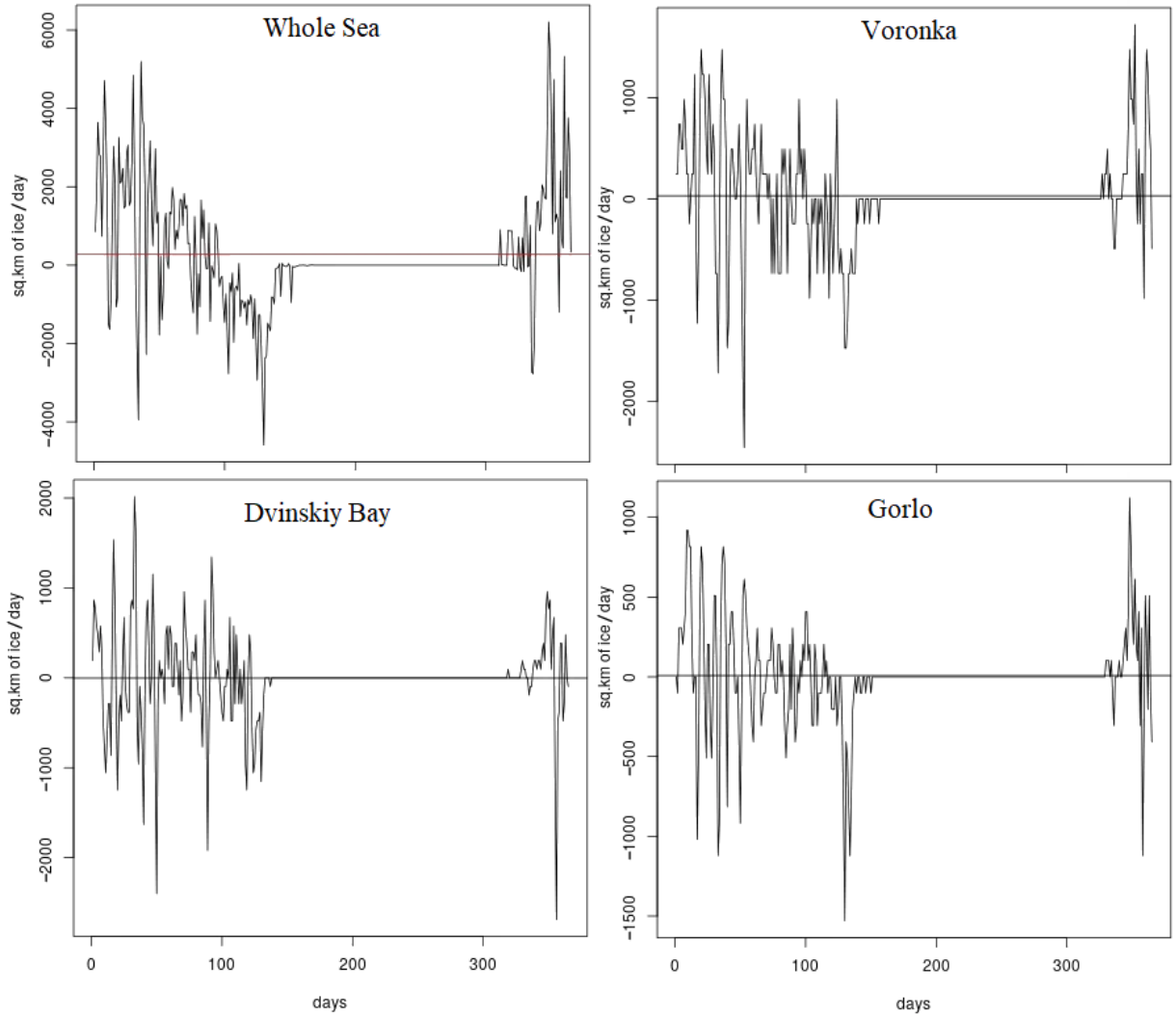

Figure 3. Freezing and melting of ice in the sea region during a year, km^2/day.

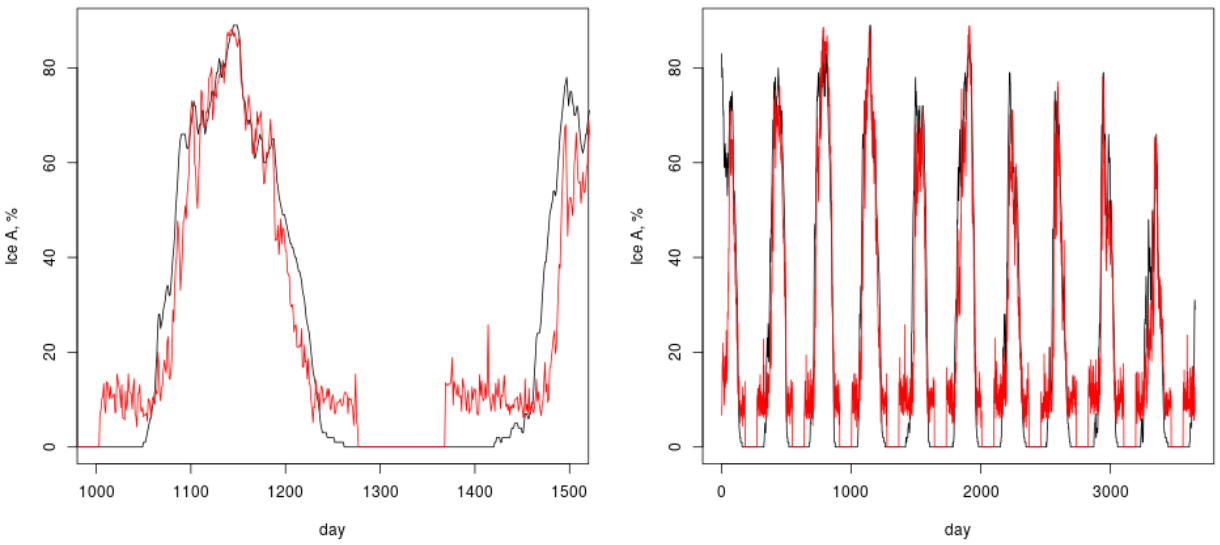

Figure 4. Daily sea-ice concentration for the White Sea for the time-span 2008–2017 (**left side**) and about one year (days 1000–1500, starting from 1 January 2008) (**right side**). The red curve is for the data, the black one is for the model.

Figure 4 also shows that, for both the model and the satellite data, ice formation starts in December and the sea is mostly ice-covered by January. The ice concentration reaches its maximum in February, melting starts in the second part of April and becomes very fast in May. The sea is ice-free in the beginning of June. These results agree well with earlier studies based on aerial reconnaissance of sea ice and data from 25 hydrometeorological stations for the years 1951–1985.

4. Conclusions

Theoretical understanding of the winter regime of the White Sea, such as the weakening of the intensity of currents, the timing of ice formation and destruction, and the removal of ice fields from the bays of the sea, is confirmed by numerical experiments. The results of the analysis of satellite images over a period of 10 years made it possible to verify the model. Each bay of the White Sea has its own regularities for the duration of the ice regime and the features of ice melting and removal to other areas of the sea, which are demonstrated by numerical simulation.

The discrepancy between satellite and model data at the beginning of the ice formation process and at the very end of the winter period of each year can be explained by the features of the "NASA Team" algorithm, which does not take into account edge pixels due to low spatial resolution. The maximum errors are observed in Kandalakshskiy Bay, which has the most indented coasts, contains many closed and semi-closed bays, and is where the ice forms first and melts last.

Supplementary Materials: The following supporting information can be downloaded at: https://www.mdpi.com/article/10.3390/fluids7100324/s1, Supplementary: Governing Equations of Sea-Water and Ice.

Author Contributions: Conceptualization, I.C. and A.T.; methodology, A.T. and V.B.; software, N.I. and I.C.; validation, A.T.; formal analysis, V.B.; data curation, V.B.; writing—original draft preparation, I.C. and V.B.; writing—review and editing, I.C and A.T.; visualization, I.C.; project administration, A.T.; funding acquisition, A.T. All authors have read and agreed to the published version of the manuscript.

Funding: The study was funded through Russian Science Foundation grant No. 22-27-20014, implemented in collaboration with Republic of Karelia authorities, with funding from the Republic of Karelia Venture Capital Fund; N.Iakovlev (sea ice model development) was supported by Russian Science Foundation grant 21-71-30023; I. Chernov worked under state order to the KRC.

Data Availability Statement: Not applicable.

Conflicts of Interest: The authors declare no conflict of interest.

Abbreviations

The following abbreviations are used in this manuscript:

AOMIP	Arctic Ocean Intercomparison Program;
BFM	Biogeochemical Flux Model;
CICE	The Los Alamos Sea Ice Model ("Sea ICE");
FCT-TG	Finite-Element Flux Corrected Taylor–Galerkin Scheme;
FEMAO	Finite-Element Model of the Arctic Ocean;
FESIM	Finite-Element Sea Ice Model;
FESOM	Finite Element Sea Ice-Ocean Model;
INM	Institute of Numerical Mathematics of RAS;
KRC	Karelian Research Centre of RAS;
MOM	Module Ocean Model;
NASA	National Aeronautics and Space Administration;
NCEP	National Centers for Environmental Prediction, USA;
NOAA	National Oceanic and Atmospheric Administration, USA;
NSIDC	National Snow and Ice Data Center, USA;

SMMR	Scanning Multichannel Microwave Radiometer;
SSM/I	Special Sensor Microwave Imager;
SSMIS	Special Sensor Microwave Imager/Sounder;
DMSP	Defense Meteorological Satellite Program;
RAS	Russian Academy of Sciences.

References

1. Filatov, N.; Pozdnyakov, D.; Johannessen, O.; Pettersson, L.; Bobylev, L. *White Sea, Its Marine Environment and Ecosystem Dynamics Influenced by Global Change*; Springer-Praxis: London, UK, 2005.
2. Lisitsyn, A.; Nemirovskaya, I.; Shevchenko, V.; Vorontsova, V. (Eds.) *White Sea System*; Scientific World: Moscow, Russia, 2017; Volumes I–IV. (In Russian)
3. Comiso, J.C.; Meier, W.; Gersten, R. Variability and trends in the Arctic Sea ice cover: Results from different techniques. *J. Geophys. Res.* **2017**, *N122*, 6883–6900. [CrossRef]
4. Andrews, J.; Babb, D.; Barger, D. Climate change and sea ice: Shipping in Hudson Bay, Hudson Strait, and Foxe Basin (1980–2016). *Elem. Sci. Anthr.* **2018**, *N6*, 1–23. [CrossRef]
5. Baklagin, V. Spatio-temporal regularities of the White Sea ice regime formation. *Adv. Oceanogr. Limnol.* **2022**, *13*, 9849. [CrossRef]
6. Zabolotskikh, E. Review of methods to retrieve sea-ice parameters from satellite microwave radiometer data. *Izv. Atmos. Ocean. Phys.* **2019**, *55*, 110–128. [CrossRef]
7. Tschudi, M.; Meier, W.; Stewart, J. An enhancement to sea ice motion and age products at the National Snow and Ice Data Center (NSIDC). *Cryosphere* **2020**, *14*, 1519–1536. [CrossRef]
8. Kern, S.; Lavergne, T.; Notz, D.; Pedersen, L.; Tonboe, R. Satellite passive microwave sea-ice concentration data set inter-comparison for Arctic summer conditions. *Cryosphere* **2020**, *14*, 2469–2493. [CrossRef]
9. Shalina, E. Regional peculiarities of changes in the ice situation in the seas of the Russian Arctic and on the route of the Northern Sea Route according to satellite observations. *Curr. Probl. Remote Sens. Earth Space* **2021**, *18*, 201–213. (In Russian)
10. Shalina, E.; Johannessen, O.; Bobylev, L. Changes in the Arctic ice cover according to satellite passive microwave sensing data from 1978 to 2007. *Curr. Probl. Remote Sens. Earth Space* **2008**, *2*, 203–228. (In Russian)
11. Cavalieri, D.; Parkinson, C. Arctic sea ice variability and trends, 1979–2010. *Cryosphere* **2012**, *6*, 881–889. [CrossRef]
12. Shalina, E. Reduction of the Arctic ice cover according to satellite passive microwave sensing. *Curr. Probl. Remote Sens. Earth Space* **2013**, *10*, 328–336. (In Russian)
13. Stroeve, J.; Notz, D. Changing state of Arctic sea ice across all seasons. *Environ. Res. Lett.* **2018**, *13*, 103001. doi: 10.1088/1748-9326/aade56. [CrossRef]
14. Johannessen, O.; Aleksandrov, V.; Frolov, I.; Sandven, S.; Pettersson, L.; Bobylev, L.; Kloster, K.; Smirnov, V.; Mironov, E.; Babich, N. *Remote Sensing of Sea Ice on the Northern Sea Route: Study and Application*; Scientific Research in the Arctic; Nauka: Saint Petersburg, Russia, 2007; Volume 3. (In Russian)
15. Gluhovskiy, B.; Terziev, F. (Eds.) The White Sea. Reference book "Seas of the USSR". In *Hydrometeorology and Hydrochemistry of Seas of the USSR, Volume II, N.2: Hydrochemical Conditions and Oceanological Base for Bioproductivity*; Hydrometeoizdat: Leningrad, Russia, 1991. (In Russian)
16. Dobrovol'skij, A.; Zalogin, B. *Seas of the USSR*; Moscow State University: Moscow, Russia, 1982. (In Russian)
17. Vihma, T.; Haapala, J. Geophysics of sea ice in the Baltic Sea: A review. *Prog. Oceanogr.* **2009**, *80*, 129–148. doi: 10.1016/j.pocean.2009.02.002. [CrossRef]
18. Zalesny, V.B.; Gusev, A.V.; Ivchenko, V.O.; Tamsalu, R.; Aps, R. Numerical model of the Baltic Sea circulation. *Russ. J. Numer. Anal. Math. Model.* **2013**, *28*, 85–100. [CrossRef]
19. Soomere, T. Numerical simulations of wave climate in the Baltic Sea: A review. *Oceanologia* **2022**. [CrossRef]
20. Haapala, J.; Meier, H.M.; Rinne, J. Numerical Investigations of Future Ice Conditions in the Baltic Sea. *AMBIO J. Hum. Environ.* **2001**, *30*, 237–244. [CrossRef]
21. Semenov, E.; Bulatov, M. Analysis of the Operative Model of Hydrophysical Field Results in the White Sea from July to August 2008. *Dokl. Earth Sci.* **2010**, *432*, 710–714. [CrossRef]
22. Chernov, I.; Lazzari, P.; Tolstikov, A.; Kravchishina, M.; Iakovlev, N. Hydrodynamical and biogeochemical spatiotemporal variability in the White Sea: A modeling study. *J. Mar. Syst.* **2018**, *187*, 23–35. [CrossRef]
23. Iakovlev, N. On the simulation of temperature and salinity fields in the Arctic Ocean. *Izv. Atmos. Ocean. Phys.* **2012**, *48*, 86–101. [CrossRef]
24. Vichi, M.; Lovato, T.; Butenschön, M.; Tedesco, L.; Lazzari, P.; Cossarini, G.; Masina, S.; Pinardi, N.; Solidoro, C.; Zavatarelli, M. *The Biogeochemical Flux Model (BFM): Equation Description and User Manual*; BFM Report Series 1.2, BFM Version 5.2; CMCC: Bologna, Italy, 2020.
25. Perezhogin, P.; Chernov, I.; Iakovlev, N. Advanced parallel implementation of the coupled ocean–ice model FEMAO (version 2.0) with load balancing. *Geosci. Model Dev.* **2021**, *14*, 843–857. [CrossRef]
26. Mellor, G.; Yamada, T. Development of a turbulence closure model for geophysical fluid problems. *Rev. Geophys. Space Phys.* **1982**, *20*, 851–875. [CrossRef]

27. Craig, P.; Banner, M. Modeling wave-enhanced turbulence in the ocean surface layer. *J. Phys. Oceanogr.* **1994**, *24*, 2546–2559. [CrossRef]
28. Mellor, G.; Blumberg, A. Wave Breaking and Ocean Surface Layer Thermal Response. *J. Phys. Oceanogr.* **2004**, *34*, 693–698. [CrossRef]
29. Griffies, S.; Gnanadesikan, A.; Pacanowski, R.; Larichev, V.; Dukowicz, J.; Smith, R. Isoneutral diffusion in a z-coordinate ocean model. *J. Phys. Oceanogr.* **1998**, *28*, 805–830. [CrossRef]
30. Gent, P.; McWilliams, J. Isopycnal mixing in ocean circulation models. *J. Phys. Oceanogr.* **1990**, *20*, 150–155. [CrossRef]
31. Visbeck, M.; Marshall, J.; Haine, T.; Spall, M. Specification of eddy transfer coeffcients in coarse resolution ocean circulation models. *J. Phys. Oceanogr.* **1997**, *27*, 381–402. [CrossRef]
32. Nurser, A.; Bacon, S. The Rossby radius in the Arctic Ocean. *Ocean Sci.* **2014**, *10*, 967–975. [CrossRef]
33. Flather, R. A tidal model of the northwest European continental shelf. *Mem. Soc. R. Sci. Liege* **1976**, *6*, 141–164.
34. Wang, Q.; Danilov, S.; Sidorenko, D.; Timmermann, R.; Wekerle, C.; Wang, X.; Jung, T.; Schr oter, J. The Finite Element Sea Ice-Ocean Model (FESOM) v.1.4: Formulation of an ocean general circulation model. *Geosci. Model Dev.* **2014**, *7*, 663–693. [CrossRef]
35. Danilov, S.; Wang, Q.; Timmermann, R.; Iakovlev, N.; Sidorenko, D.; Kimmritz, M.; Jung, T.; Schroter, J. Finite-Element Sea Ice Model (FESIM), version 2. *Geosci. Model Dev.* **2015**, *8*, 1747–1761. [CrossRef]
36. Hunke, C.; Lipscomb, W.; Turner, A.; Jeffery, N.; Elliott, S. *CICE: The Los Alamos Sea Ice Model, Documentation and Software, Version 5.0*; Los Alamos National Laboratory Technical Report LA-CC-06-012; Los Alamos National Laboratory: Los-Alamos, NM, USA, 2013.
37. Loehner, R.; Morgan, K.; Peraire, J.; Vahdati, M. Finite element flux-corrected transport (FEM-FCT) for the Euler and Navier-Stokes equations. *Int. J. Numer. Meth. Fluids* **1987**, *7*, 1093–1109. [CrossRef]
38. Semtner, A. A model for the thermodynamic growth of sea ice in numerical investigations of climate. *J. Phys. Oceanogr.* **1976**, *6*, 379–389. [CrossRef]
39. Ridders, C. A new algorithm for computing a single root of a real continuous function. *IEEE Trans. Circuits Syst.* **1979**, *CAS26*, 979–980. [CrossRef]
40. Kalnay, E.; Kanamitsu, M.; Kistler, R.; Collins, W.; Deaven, D.; Gandin, L.; Iredell, M.; Saha, S.; White, G.; Woollen, J.; et al. The NCEP/NCAR 40-year reanalysis project. *Bull. Am. Meteorol. Soc.* **1996**, *77*, 437–470. [CrossRef]
41. Griffies, S. *Elements of MOM4p1, GFDL Ocean Group Technical Report No. 6*; Technical Report; NOAA/Geophysical Fluid Dynamics Laboratory: Princeton, NJ, USA, 2009.
42. Chernov, I.; Tolstikov, A. The White Sea: Available Data and Numerical Models. *Geosci. Model Dev.* **2020**, *10*, 463. [CrossRef]